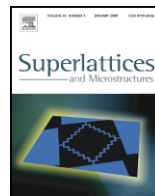




ELSEVIER

Contents lists available at ScienceDirect

## Superlattices and Microstructures

journal homepage: [www.elsevier.com/locate/superlattices](http://www.elsevier.com/locate/superlattices)

## Study of optical properties of electrospun light-emitting polymer fibers

S. Pagliara<sup>a,b,\*</sup>, A. Camposeo<sup>a</sup>, F. Di Benedetto<sup>a</sup>, A. Polini<sup>a,b</sup>, E. Mele<sup>a</sup>,  
L. Persano<sup>a</sup>, R. Cingolani<sup>a,b</sup>, D. Pisignano<sup>a,b</sup>

<sup>a</sup> NNL, National Nanotechnology Laboratory of Istituto Nazionale di Fisica della Materia–Consiglio Nazionale delle Ricerche, Università del Salento, via Arnesano, 73100 Lecce, Italy

<sup>b</sup> Scuola Superiore ISUFI, Università del Salento, via Arnesano, 73100 Lecce, Italy

### ARTICLE INFO

#### Article history:

Available online 11 August 2009

#### Keywords:

Waveguiding  
Gain polymer fibers  
Lasing-emission

### ABSTRACT

We realize light-emitting polymer fibers based on both optically inert polymers doped by molecules exhibiting optical gain and optically active conjugated polymers. Waveguiding properties of the produced polymer structures are demonstrated, with a loss coefficient of around  $10^3 \text{ cm}^{-1}$ . We also find that single polymer fibers doped with gain molecules form Fabry–Pérot cavities, showing photoluminescence spectra with modes equally spaced by 1.7 nm. Coherent emission is demonstrated from fibers made upon increasing the excitation fluence above threshold values of the order of a few tens of  $\mu\text{J}/\text{cm}^2$ .

© 2009 Elsevier Ltd. All rights reserved.

### 1. Introduction

In recent years linear photonic nanostructures, both organic and inorganic, [1] have been the subject of intense investigation as building blocks for generation, confinement, guiding, and detection of light. In particular, a novel and interesting class of 1-dimensional photonic nanostructures well-suited for nanophotonics is represented by polymer nanofibers [2], which show unique features in terms of high structural and chemical flexibility and low fabrication cost. These fibers can be realized by electrostatic spinning that, compared to other production technologies [3–5], permits processing of large volumes through the plastic stretching of polymer solutions by the applied electric field [6–9]. The electrospinning is a high-throughput method which applies to a polymeric solution of suitable concentration. This technology relies on different stages, including the formation of a charged jet

\* Corresponding author at: NNL, National Nanotechnology Laboratory of Istituto Nazionale di Fisica della Materia–Consiglio Nazionale delle Ricerche, Università del Salento, via Arnesano, 73100 Lecce, Italy. Tel.: +39 0832298122.

E-mail address: [stefano.pagliara@unile.it](mailto:stefano.pagliara@unile.it) (S. Pagliara).

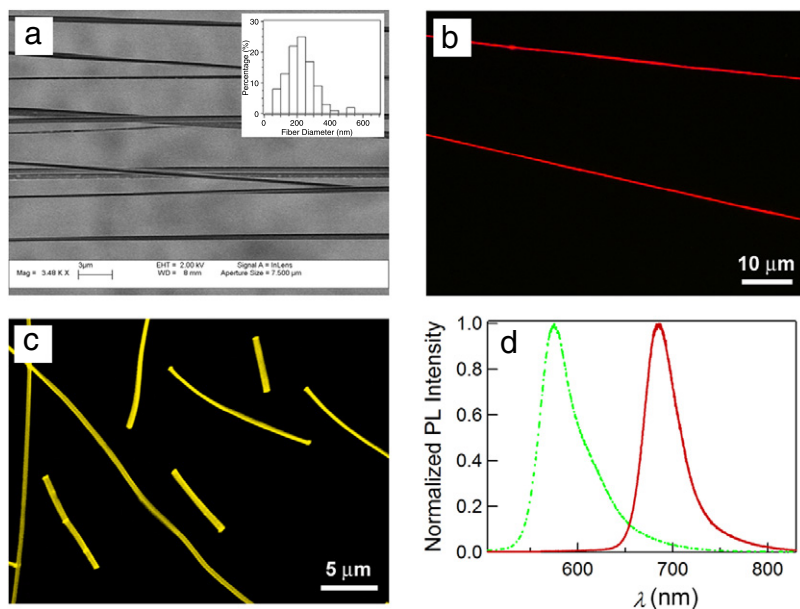


**Fig. 1.** (a) SEM micrograph of electrospun fibers. Inset: Typical distribution of fiber diameters. (b–c) Fluorescence micrographs of conjugated polymer (b) and R6G-doped (c) fibers, respectively. (d) Corresponding PL spectra. Continuous spectrum peaked at 690 nm: conjugated polymer fiber. Dashed spectrum peaked at 570 nm: R6G-doped fibers.

by means of the application of an electrostatic potential (from few to tens of kV) to the polymeric solution, the subsequent stretching and whipping processes due to the concomitant liquid surface electrostatic repulsion and solvent evaporation, and the collection of the produced fibers on a metal target. The electrospinning is affected by molecule (solution concentration and conductivity, polymer molecular weight and steric hindrance), processing (applied voltage, interelectrodes distance, solution flow-rate), and ambient-related parameters (temperature and humidity). Upon optimization, this approach allows us to produce polymeric fibers, with diameter of the order of 1  $\mu\text{m}$  down to sub-100 nm. In addition, the jet stretching promotes some degree of internal molecular orientation of the active molecules [10–12]. Here we report on the investigation of the light emission properties of electrospun fibers with diameter in the range from hundreds of nanometers to a few micrometers. Measured loss coefficients for self-waveguiding of emitted light from the polymer fibers are of the order of  $10^3 \text{ cm}^{-1}$ . Furthermore, we find that photoluminescence (PL) spectra from polymer fibers doped with gain molecules show characteristic spectral features of Fabry–Pérot cavities, that allow coherent amplification of the emitted light.

## 2. Results and discussion

The conjugated polymer fibers used in this study are electrospun from chloroform solutions of the compound, poly[ $\{2\text{-methoxy-5-(2\text{-ethylhexyloxy})-1,4-(1\text{-cyanovinylphenylene})\}\text{-co-}\{2,5\text{-bis(N,N'-diphenylamino)-1,4-phenylene}\}$ ] with concentration in the range  $10^{-6}$ – $10^{-4}$  M. Other fibers are instead electrospun by a solution of Rhodamine 6G (R6G, 0.2–0.5 wt%) dissolved in  $10^{-3}$  M chloroform solutions of poly(methyl methacrylate) (PMMA).

The resulting electrospun fibers exhibit diameters in the range 100–3000 nm, depending on the solution concentration and on other process parameters, including applied bias voltage [13], solution feeding flow [14], and needle-collector distance [15], as we find by scanning electron microscopy (SEM, Fig. 1a). In particular, the inset of Fig. 1a displays a typical distribution of fiber diameters, centered around 200 nm, which is obtained for applied bias voltage of 24 kV, solution feeding flow around  $10 \mu\text{L min}^{-1}$  and needle-collector distance of the order of 10 cm.

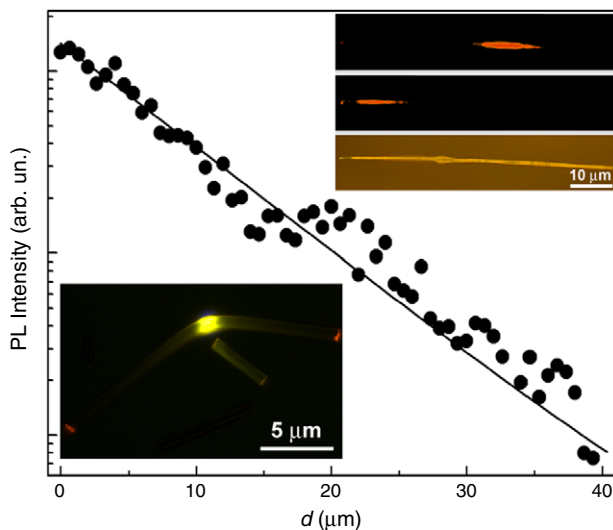


**Fig. 2.** Intensity of the self-emitted guided light inside a single polymer fiber vs. distance ( $d$ ) between the fiber tip and the exciting laser spot. The superimposed continuous line is the best fit of the data to an exponential decay equation. Insets: optical micrographs of the waveguiding in single polymer fibers (see the text).

Fluorescence micrographs of the fabricated light-emitting fibers show uniform emission from both conjugated polymer (Fig. 1b) and doped samples (Fig. 1c). The PL spectra (Fig. 1d) from the red-emitting polymer (continuous line) and R6G doped (green line) fiber mats do not show remarkable differences with respect to the corresponding spin-cast films. Slight blue shifts (5–8 nm) are observed in the peak wavelength of the conjugated polymer fibers. These differences arise from the suppression of exciton migration toward low-energy chromophores due to the packing geometry induced by the electrospinning process [15]. Since the refractive index of the polymer species used for the fabrication of the fibers (1.5–1.7) is significantly larger than the surrounding medium (mostly air), these polymer elements can constitute quite effective waveguides for the self-emitted light. We characterize the propagation loss of such waveguides, by exciting a single red-emitting polymer fiber (left inset of Fig. 2) with a tightly focused laser beam (excitation wavelength = 405 nm and spot diameter around 8  $\mu\text{m}$ ). We then measure the integrated PL intensity emitted from the tip of the fiber upon varying the distance,  $d$ , between the excitation spot and the fiber tip. The right inset of Fig. 2 shows—from bottom to top—a bright-field micrograph of a single light-emitting fiber and corresponding fluorescence images evidencing the bright-light spots exiting the fiber endpoint for  $d$  equal to 50 and 200  $\mu\text{m}$  respectively. The resulting dependence of the waveguided intensity on  $d$  is shown in Fig. 2, also displaying the best fit to the experimental data by the exponential decay equation:

$$I = I_0 e^{-\gamma d}. \quad (1)$$

The fit provides a value of about  $1.3 \times 10^3 \text{ cm}^{-1}$  for the loss coefficient  $-\gamma$ —which is comparable to those found for R6G doped fibers ( $0.2\text{--}1.2 \times 10^3 \text{ cm}^{-1}$ ) [14]. These optical losses can be determined by polymer self-absorption, and by scattering from bulk and from surface defects of the fiber [15]. We believe that self-absorption especially plays a role in increasing the optical losses. In fact, the spectra of the waveguided PL emission, i.e. collected at the fiber tip, is red-shifted compared to the emission collected vertically from the fiber surface, thus indicating the occurrence of significant self-absorption, which is more effective at higher energies.

Finally, cavity effects are investigated in the R6G-doped polymer fibers. Each segmented fiber can form a Fabry–Pérot cavity which allows spectral selection and light amplification, because of the high confinement of the emitted light. In particular, for a cylindrical cavity of length,  $L$ , and central

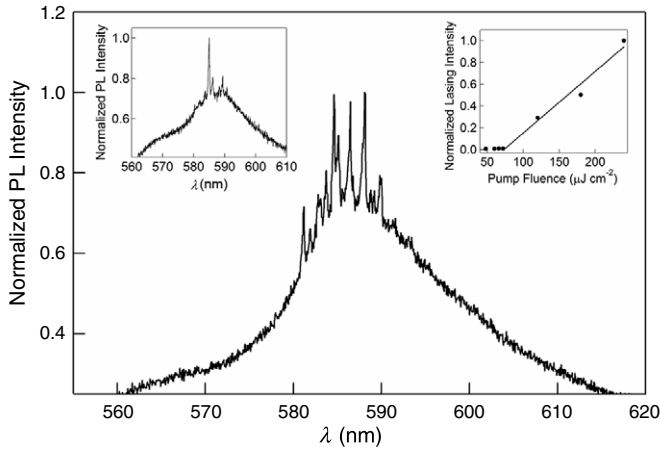


**Fig. 3.** PL spectrum from a single fiber with modes equally spaced by 1.7 nm. Left inset: single-mode emission for pumping fluence above threshold. Right inset: Laser emission intensity vs. excitation fluence. The continuous line is a fit to the data in the above-threshold linear region of the input–output characteristic.

wavelength,  $\lambda_c$ , the mode spacing,  $\Delta\lambda_c$  is given by:

$$\Delta\lambda_c = \left( \frac{\lambda_c^2}{2L} \right) \left( n - \lambda_c \left. \frac{dn}{d\lambda} \right|_{\lambda_c} \right)^{-1} \quad (2)$$

where  $dn/d\lambda$  indicates the refractive index dispersion. Indeed, by characterizing the emission from the tip of single segmented fibers with lengths in the range 10–100  $\mu\text{m}$ , we find evidence of equally-spaced modes (Fig. 3). The measured mode spacing is around 1.7 nm, corresponding to an estimated fiber length of about 70  $\mu\text{m}$  (Eq. (2)). This value is in accordance with the measured segment length. Modes are observed only in spectra collected from the segment tips, whereas we do not record any modes in spectra collected from the body of the fibers. These findings support the attribution of such spectral features to Fabry–Perot cavity modes rather than to whispering gallery modes, usually observed in the plane perpendicular to the axis of a cylindrical cavity [16]. Moreover, probably due to the large surface (up to thousands of  $\text{m}^2$  per gram) of gain medium directly exposed to oxygen and moisture atmosphere in the nanofibers, which is known to cause quenching of the emission in conjugated polymers [17], we do not routinely observe cavity modes in fibers made by these organic semiconductor materials.

Single-fiber microcavities are particularly promising for being exploited for coherent light amplification. The lasing performances of single polymer fibers are evaluated by exciting each single fiber by the second harmonic of a Nd:YAG microlaser (532 nm, pulse duration 0.6 ns, repetition rate 100 Hz) and collecting the PL signal from the fiber tips. We find that, by increasing the pumping fluence above a threshold value (75  $\mu\text{J cm}^{-2}$ ), one can observe a significant increase of the emission from a single mode with respect to other modes (inset of Fig. 3), in accordance with the occurrence of coherent amplification of the emitted light, and of lasing. Further work on embedding active polymer fibers in different lasing geometries is currently ongoing in our laboratory.

### 3. Conclusion

The electrospinning technology provides a simple and low cost method to realize flexible, fully organic, light emitting fibers suitable for the integration in photonics devices. Specifically, we have investigated the emission and waveguiding properties of conjugated polymer fibers measuring loss coefficients of the order of  $10^3 \text{ cm}^{-1}$ . Moreover we have found evidence of cavity effects in composite polymer fibers, which are particularly promising in view of applications requiring coherent, lasing emission.

## Acknowledgement

This work was partially supported by the FIRB Contract RBIP06SH3W.

## References

- [1] Y. Xia, P. Yang, Y. Sun, Y. Wu, B. Mayers, B. Gates, Y. Yin, F. Kim, H. Yan, *Adv. Mater.* 15 (2003) 353.
- [2] D. Li, Y. Xia, *Adv. Mater.* 16 (2004) 1151.
- [3] F. Quochi, F. Cordella, A. Mura, G. Bongiovanni, F. Balzer, H.-G. Rubahn, *Appl. Phys. Lett.* 88 (2006) 041106.
- [4] J. Liu, E. Sheina, T. Kowalewski, R.D. McCullough, *Angew. Chem. Int. Ed.* 41 (2002) 329.
- [5] A. Noy, A.E. Miller, J.E. Klare, B.L. Weeks, B.W. Woods, J.J. DeYoreo, *Nano Lett.* 2 (2002) 109.
- [6] D.H. Reneker, I. Chun, *Nanotechnology* 7 (1996) 216.
- [7] A.G. MacDiarmid, W.E. Jones Jr., I.D. Norris, J. Gao, A.T. Johnson Jr., N.J. Pinto, J. Hone, B. Han, F.K. Ko, H. Okuzaki, M. Llaguno, *Synth. Met.* 119 (2001) 27.
- [8] Y. Dzenis, *Science* 304 (2004) 1917.
- [9] J.M. Moran-Mirabal, J.D. Slinker, J.A. DeFranco, S.S. Verbridge, R. Ilic, S. Flores-Torres, H. Abruña, G.G. Malliaras, H.G. Craighead, *Nano Lett.* 7 (2007) 458.
- [10] A. Bianco, G. Iardino, A. Manuelli, C. Bertarelli, G. Zerbi, *Chem. Phys. Chem.* 8 (2007) 510.
- [11] T. Kongkhlang, K. Tashiro, M. Kotaki, S. Chirachanchai, *J. Am. Chem. Soc.* 130 (2008) 15460.
- [12] L.M. Bellan, H.G. Craighead, *Polymer* 49 (2008) 3125.
- [13] A. Camposeo, F. Di Benedetto, R. Stabile, R. Cingolani, D. Pisignano, *Appl. Phys. Lett.* 90 (2007) 143115.
- [14] A. Camposeo, F. Di Benedetto, R. Stabile, A.A.R. Neves, R. Cingolani, D. Pisignano, *Small* 5 (2009) 562.
- [15] F. Di Benedetto, A. Camposeo, S. Pagliara, E. Mele, L. Persano, R. Stabile, R. Cingolani, D. Pisignano, *Nat. Nanotechnology* 3 (2008) 614.
- [16] A. Shevchenko, K. Lindfors, S.C. Buchter, M. Kaivola, *Opt. Commun.* 245 (2005) 349.
- [17] M. Yan, L.J. Rothberg, F. Papadimitrakopoulos, M.E. Galvin, T.M. Miller, *Phys. Rev. Lett.* 73 (1994) 744.